

D. SUPPLEMENTARY MATERIAL

RADIATIVE QUENCHING
of
 $^3\text{He}^+$ IONS
from
MIXTURES with H_2 MOLECULES

$^3\text{He}^+ / ^4\text{He}^+$ isotope effects

Radiative decay of ${}^3\text{He}^+$ versus ${}^4\text{He}^+$ ions from mixtures with para- and ortho- H_2

Fig. D1. Partial yield functions $p^{\text{rad},c}(E; J, p)$ for $c=p,o$

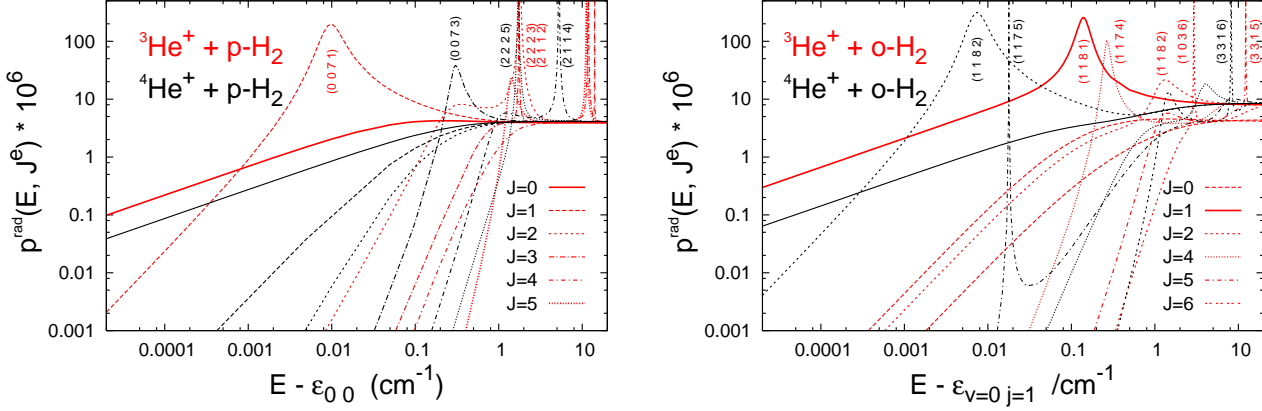
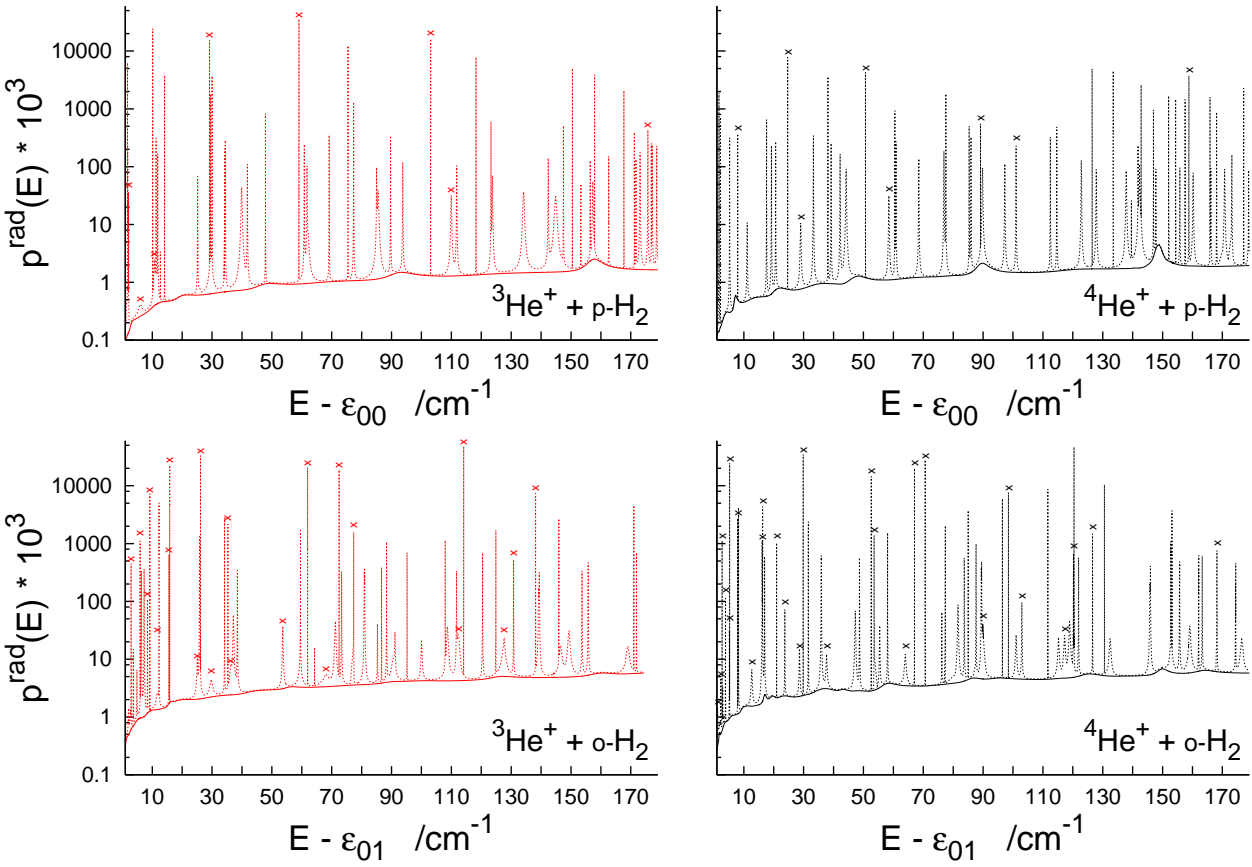


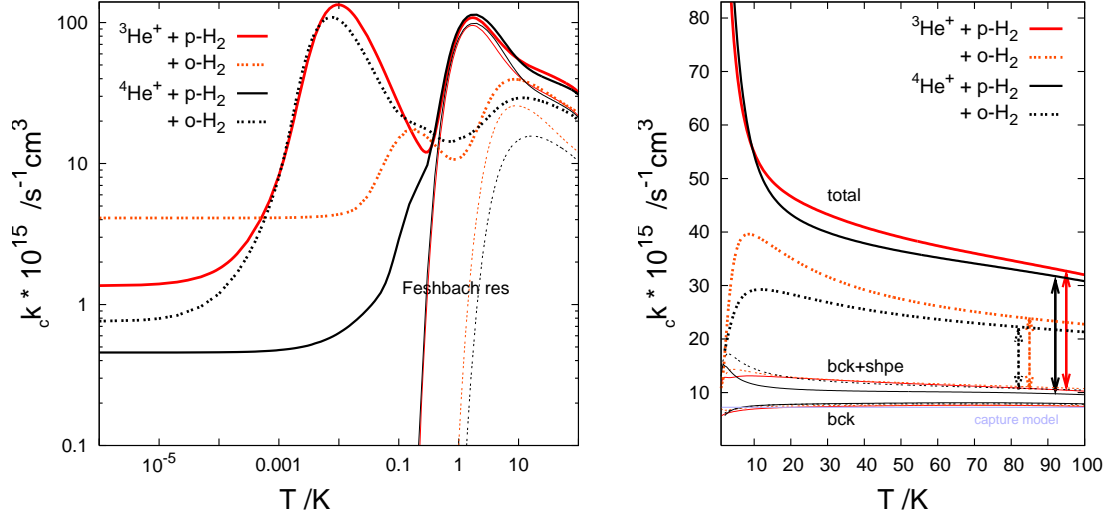
Fig. D2. Total yield functions $p^{\text{rad},c}(E)$



Crosses mark shape resonances

There is no major difference between the ${}^3\text{He}^+ - \text{c-H}_2$ and ${}^4\text{He}^+ - \text{c-H}_2$ systems in the average resonance density in the entire energy intervals shown in Fig. 2. However, as shown in Fig. 1, the overall shift of the rovibrational energy levels in the lighter systems causes important changes in the near-threshold regions. Some levels bound in ${}^4\text{He}^+ - \text{c-H}_2$, like (0 0 71) and (1 1 8 1), become shape resonances in ${}^3\text{He}^+ - \text{c-H}_2$. In turn, the near-threshold resonances in ${}^4\text{He}^+ - \text{o-H}_2$, like (1 1 8 2), leave this region in ${}^3\text{He}^+ - \text{o-H}_2$.

Fig. D3. Rate constants ${}_c k(T)$ for $c=p,o$



COMMENTS

The comparison of the rate constant functions for the reaction in the mixtures with the ${}^3\text{He}^+$ and the ${}^4\text{He}^+$ ions, the red versus black lines in Figs. 3 and 4, shows effects which one actually expects after having seen the resonance structures in Figs. 1 and 2, namely:

- (i) substantial differences in magnitude and shape of the functions in the cold temperature range, $T < 0.1 \text{ K}$, and
- (ii) rather small changes in the $\sim 1 - 100 \text{ K}$ range.

In the latter range, transitions from the rotational Feshbach resonances are the rate determining factors. The number and strength of these transitions depend primarily on the diatomic reagents, only H_2 here.

Fig. 5 and Table DI summarize the ${}^3\text{He}^+ \rightarrow {}^4\text{He}^+$ substitution effects on the functions $k(T)$ and $k_{\text{nrm}}(T)$. They should be compared with Fig. C7c and Table IX in the main text which give analogous information on the $\text{D}_2 \rightarrow \text{H}_2$ substitution. Differences between effects of the two substitutions are obviously much more pronounced in the cold range than in the subthermal range. However, the quantitative estimations of the effects in the subthermal range are more reliable as they are definitely less sensitive to possible inaccuracies of the used PES.

Radiative decay of ${}^3\text{He}^+$ versus ${}^4\text{He}^+$ ions from mixtures with equilibrium and normal H_2

Fig. D4. Rate constant functions $k(T)$.

Resonance and background contributions

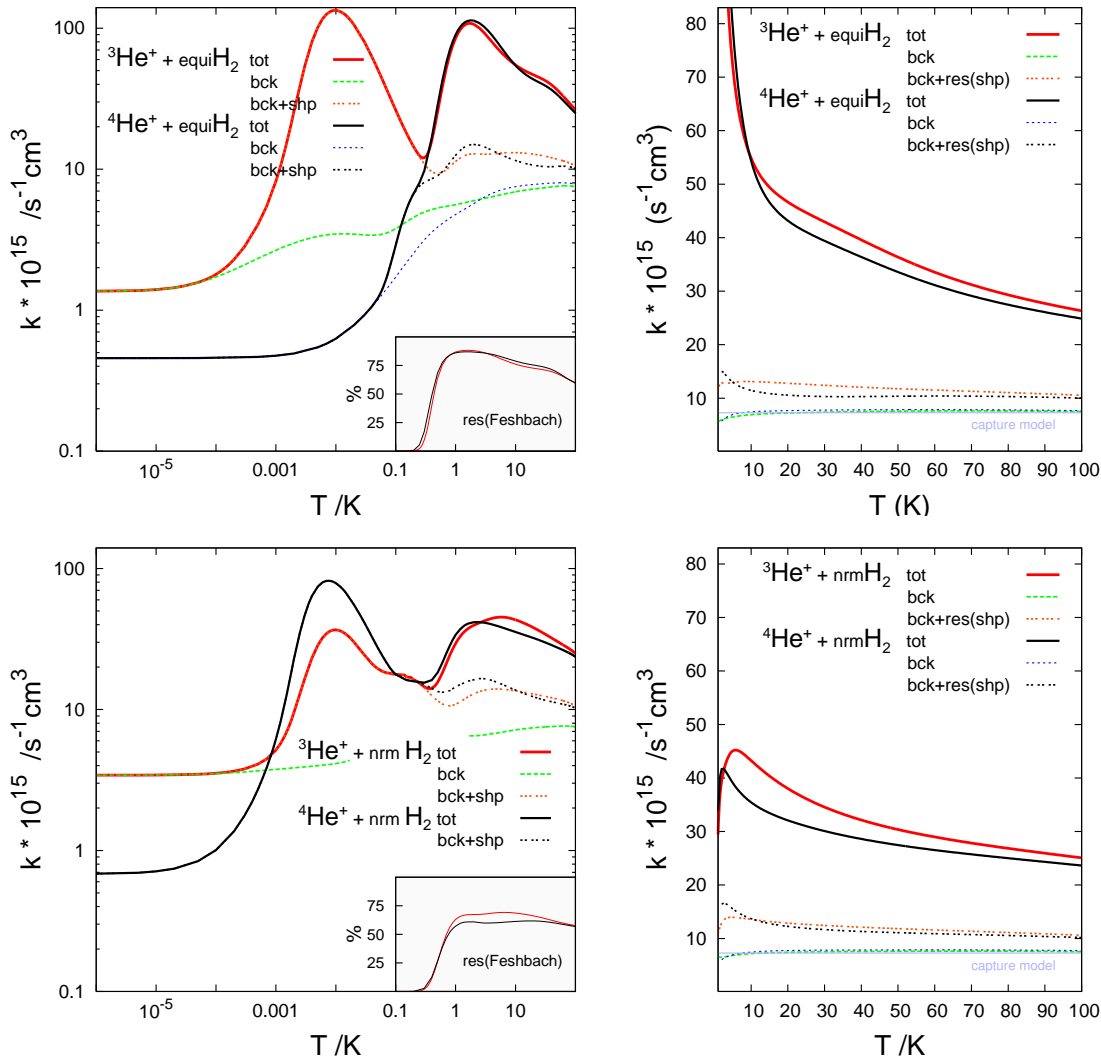


Fig. D5. ${}^3\text{He}/{}^4\text{He}$ isotope effect on $k(T)$

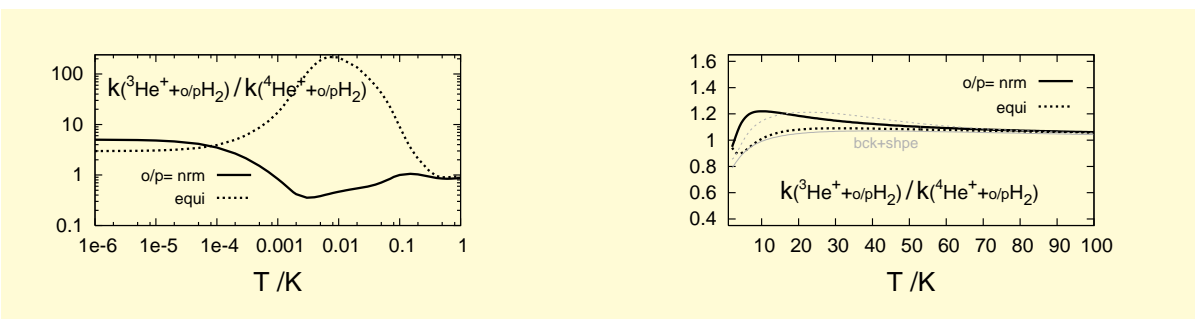


TABLE DI: Rate constants $k(T)$ (in $10^{-15} \text{ s}^{-1}\text{cm}^3$) for radiative quenching of ${}^3\text{He}^+$ ions from gas mixtures with equilibrium and normal hydrogen at selected temperature values in the range 10^{-6} –100 K compared to the rate constants for quenching of the ${}^4\text{He}^+$ ions, cf. Table IX.

${}^3\text{He}^+ + \text{H}_2$				$\frac{{}^3\text{He}^+ + \text{H}_2}{{}^4\text{He}^+ + \text{H}_2}$				${}^3\text{He}^+ + \text{H}_2$				$\frac{{}^3\text{He}^+ + \text{H}_2}{{}^4\text{He}^+ + \text{H}_2}$			
T	equi	nrm		equi	nrm		equi	nrm		equi	nrm		equi	nrm	
10^{-6}	1.36	3.42		2.97	5.02		2	106.7	39.6		0.94	0.95			
10^{-5}	1.40	3.43		3.06	4.83		3	92.6	42.5		0.91	1.03			
0.0001	1.79	3.53		3.91	3.50		4	80.3	44.3		0.90	1.10			
0.001	8.21	5.15		17.3	0.84		5	72.0	45.1		0.91	1.16			
0.002	25.65	9.52		52.0	0.42		6	66.3	45.2		0.93	1.18			
0.005	101.60	28.56		186.4	0.38		7	62.2	44.9		0.95	1.20			
0.01	133.89	36.74		213.3	0.47		8	59.1	44.6		0.97	1.21			
0.02	106.07	30.16		135.6	0.54		10	54.9	43.3		1.01	1.22			
0.03	79.96	24.37		86.5	0.59		15	49.4	40.4		1.06	1.21			
0.05	51.20	19.50		42.2	0.71		20	46.7	38.0		1.08	1.18			
0.08	32.57	18.08		16.0	0.91		30	42.8	34.6		1.09	1.15			
0.10	26.26	17.77		9.6	1.00		40	39.9	32.1		1.09	1.12			
0.30	12.05	14.50		1.23	0.93		50	36.4	30.3		1.08	1.11			
0.50	25.58	15.59		0.90	0.85		60	33.5	29.0		1.08	1.09			
0.60	38.49	18.17		0.90	0.84		70	31.2	27.9		1.07	1.08			
0.80	64.98	24.27		0.93	0.86		80	29.3	26.8		1.07	1.07			
1.00	85.25	29.45		0.94	0.87		90	27.7	25.9		1.06	1.07			
1.40	105.01	35.67		0.96	0.91		100	26.3	25.1		1.06	1.06			